Optical Engineering

OpticalEngineering.SPIEDigitalLibrary.org

Investigation of Yb-doped $LiLuF_4$ single crystals for optical cooling

Azzurra Volpi
Giovanni Cittadino
Alberto Di Lieto
Arlete Cassanho
Hans P. Jenssen
Mauro Tonelli

SPIE.

Azzurra Volpi, Giovanni Cittadino, Alberto Di Lieto, Arlete Cassanho, Hans P. Jenssen, Mauro Tonelli, "Investigation of Yb-doped $LiLuF_4$ single crystals for optical cooling," *Opt. Eng.* **56**(1), 011105 (2016), doi: 10.1117/1.OE.56.1.011105.

Investigation of Yb-doped $LiLuF_4$ single crystals for optical cooling

Azzurra Volpi,[a,*] Giovanni Cittadino,[a] Alberto Di Lieto,[a,b] Arlete Cassanho,[c] Hans P. Jenssen,[c] and Mauro Tonelli[a,b]
[a]Università di Pisa, Dipartimento di Fisica, Largo B. Pontecorvo 3, I-56127 Pisa, Italy
[b]NEST Istituto di Nanoscienze—CNR, Piazza S. Silvestro 12, I-56127 Pisa, Italy
[c]AC Materials, Inc., 756 Anclote Road, Tarpon Springs, Florida 34689, United States

Abstract. Optical cooling of solids, relying on annihilation of lattice phonons via anti-Stokes fluorescence, is an emerging technology that is rapidly advancing. The development of high-quality Yb-doped fluoride single crystals definitely led to cryogenic and sub-100-K operations, and the potential for further improvements has not been exhausted by far. Among fluorides, so far the best results have been achieved with Yb-doped $LiYF_4$ (YLF) single crystals, with a record cooling to 91 K of a stand-alone YLF:10%Yb. We report on preliminary investigation of optical cooling of an $LiLuF_4$ (LLF) single crystal, an isomorph of YLF where yttrium is replaced by lutetium. Different samples of 5% Yb-doped LLF single crystals have been grown and optically characterized. Optical cooling was observed by exciting the Yb transition in single-pass at 1025 nm and the cooling efficiency curve has been measured detecting the heating/cooling temperature change as a function of pumping laser frequency. [DOI: 10.1117/1.OE.56.1.011105]

Keywords: optical cooling; anti-Stokes fluorescence; rare-earth-doped materials; fluoride single crystals; $LiYF_4$; ytterbium.

Paper 161019SSP received Jun. 27, 2016; accepted for publication Aug. 1, 2016; published online Oct. 5, 2016.

1 Introduction

Optical cooling of solids is based on the process of anti-Stokes fluorescence, where laser excitation tuned above the mean emission wavelength of the electronic transition induces spontaneous emission of blue-shifted photons. The extra energy is supplied by annihilation of lattice phonons, occurring to restore the equilibrium distribution of the electronic excitations generated. Because in the solid-phase thermal energy is mostly contained in the vibrational modes of the lattice, i.e., lattice phonons, anti-Stoke photons, which exit the material, remove heat from the system, resulting in a cooling process. Net bulk cooling occurs if the decay is predominantly radiative.

Since its first experimental demonstration in 1995,[1] when a Yb-doped ZBLAN glass was optically cooled 0.3 K below room temperature trough fluorescence upconversion, such technology has tremendously advanced, until reaching in the last few years cryogenic and sub-100 K temperatures.[2–5] Both optimization of material quality, in terms of structural quality and optical purity, and improvements in the experimental conditions, regarding pumping scheme and heat load management, have permitted such progresses, dramatically pushing down the minimum achievable temperatures. In terms of active media, several rare-earth-doped materials have been investigated. However, great improvements of cooling performances have been achieved only with the development of high-quality Yb-doped fluoride single crystals, which definitely led to laser cooling operations in the cryogenic and, subsequently, sub-100-K regime. Currently, the lowest temperature achieved is 91 K in a 10%Yb-doped $LiYF_4$ (YLF) single crystal optically cooled from room temperature by laser excitation of the Yb transition at 1020 nm in a Herriot cell.[5] The potential for further improvements, however, has not been exhausted by any means. Calculations indicate that operations close to the liquid nitrogen temperature can be in principle achieved by reducing impurities-mediated background absorption.[6]

Fluoride single crystals possess several favorable properties for optical cooling experiments. The main advantage of fluorides, compared to other single crystalline hosts, is the low phonon cut-off energy (~300 to 500 cm^{-1}) that effectively suppresses the rate of detrimental nonradiative relaxation processes, which prevent radiative emission through phonon release, i.e., heat dissipation in the lattice. Moreover, the fluorides possess other advantages including low refractive index (1.4 to 1.5), which reduces photon trapping via total internal reflection at the interfaces, and large transparency window in the IR (up to 7 to 10 μm). They also exhibit good thermo-mechanical properties. The thermal conductivity is typically between 4 and 7 W/mK and the mechanical hardness is between 3 and 5 Mohs.

Despite such favorable properties, due to the strong reactivity of fluorine, the growth of high-quality samples is a very critical process, which requires ultracontrolled procedures to avoid inclusions of contaminants. Inclusion of unwanted impurities strongly degrades and even compromises the anti-Stokes process causing parasitic absorption and heat-generating phonon-assisted processes, competing with the heat removal via anti-Stokes emission.

Among fluorides, so far, the best laser cooling performances were achieved with Yb-doped YLF single crystals active media. However, other fluorides have not been studied very much.[7] In this work, we report on the investigation of the $LiLuF_4$ (LLF) single crystal, an isomorph of the YLF crystal, where yttrium is replaced by lutetium. Similar to the YLF crystal, the LLF crystal possesses a tetragonal

*Address all correspondence to: Azzurra Volpi, E-mail: azzurra.volpi@df.unipi.it

0091-3286/2016/$25.00 © 2016 SPIE

crystalline structure with lattice parameters $a = 0.5130$ nm and $c = 1.055$ nm[8] and space group $I4_1/a$. In the LLF host, trivalent rare-earth ions substitute Lu^{3+} host ions, with site symmetry S_4 and coordination number 8. In several laser experiments, the replacement of yttrium by lutetium has resulted in improved laser performances, leading to better performances of LLF over its isomorph YLF both in continuous and pulsed regime.[9,10] An isomorph, the LLF crystal, appears to exhibit some advantageous properties, which distinguish the two structures. At first, conversely to YLF, the LLF crystal has a congruent melting point, typically resulting in high-bulk optical quality, and, due to the replacement of yttrium by lutetium, it exhibits a lower phonon cut-off energy. The substitution of yttrium by lutetium also affects the strength of the crystal field. The shorter effective ionic radius of Lu^{3+} compared to Y^{3+} results in a larger splitting Stark for Yb^{3+} ions in LLF host than in YLF.[11] Larger ground-state Stark splitting can be favorable for the higher temperature range but can be detrimental at low temperatures, preventing the cooling process when kT becomes smaller than the energy separation between Stark sublevels. In addition to that, the LLF crystal has the advantage of a smaller difference in thermal expansion coefficients and thermal conductivity along each axis of the crystal axes. Although pure LLF exhibits a lower thermal conductivity than YLF, it will also show a lower decrease in thermal conductivity after Yb^{3+} doping, thanks to a better matching of Yb^{3+} and Lu^{3+} in ionic mass and radius.

Although optical cooling in Yb-doped LLF single crystals has been already demonstrated,[12] in this work, we report on measurements of the intrinsic cooling efficiency curve, with evaluation of external quantum efficiency (EQE) and background absorption parameters. High-quality LLF single crystals-doped Yb at 5 at.% have been grown, optically characterized, and tested in a standard set-up. The cooling efficiency curve has been measured observing the heating/cooling temperature change as a function of pumping wavelength. EQE and background absorption parameters have been estimated from fits to experimental data.

2 Crystal Growth and Spectroscopic Characterization

2.1 *Crystal Growth and Assessment of Sample Quality*

In this work, we investigated the cooling performances of two 5 at.% Yb-doped LLF single crystals, labeled as A and B in the following. Sample A was grown at AC Material (Tarpon Spring, Florida), whereas sample B was grown at Pisa University. Both samples, however, were grown by means of the Czochralski technique[13] in similar furnaces equipped with resistive heating, optical automated diameter control, and a high-vacuum system. Binary fluoride raw materials of LuF_3, LiF, and YbF_3 with guaranteed 5 N purity (99.999%) were used as starting materials. For both samples, LuF_3 and LiF compounds were mixed in the stoichiometric ratio 1 : 1 and a proper amount of YbF_3 powders was added to obtain a 5-at.% Yb doping level. The segregation coefficient for Yb^{3+} in LLF is expected to be close to 1. Prior to melting, particular care needs to be taken in vacuuming the growth chamber to avoid interaction of fluoride raw materials with water at high temperature, which leads to formation of oxygen complexes in the melt. These complexes are the most detrimental contaminants to avoid when growing fluorides, as they efficiently substitute for F^- ions in the crystalline structure and if incorporated inside growing crystals compromise the optical quality of finished samples. Melting and growth processes were carried out under high purity (5 N) Ar and CF4 atmosphere. A minor concentration of CF4 (typically ~20% in argon) is added to prevent reduction of Yb^{3+} to the 2+ state during the melting phase. Yb^{2+} ions, indeed, besides reducing the concentration of Yb^{3+} ions in the melt, act as detrimental contaminants if incorporated inside growing crystals. During growth, the pulling rate was between 0.5 and 1.0 mm/h and the rotation rate 5 rpm. After growth, both samples were investigated by means of x-ray back-scattering diffraction to identify the orientation of the crystallographic axes for preparing oriented samples for spectroscopy and laser cooling experiments. The x-ray analysis also verified the single crystalline structure. The absence of internal defects, such as cracks, microbubbles, and dislocations, was checked from scattering analysis of visible laser beams. The absence of major contaminants, which might have been incorporated during the growth process, was checked analyzing the absorption spectrum of the two samples from the UV (200 nm) up to 2 μm. For both samples, the absorption spectra, shown in Fig. 1, did not show any spurious peak, which can be ascribed to optically active impurities, only the absorption band relative to the Yb transition $^5F_{7/2} \rightarrow F_{5/2}$ is detectable. Inclusion of hydroxyl radicals, Yb^{2+} ions and other impurities can thus be ruled out, within the sensitivity of our instrumentations (~tens of ppm), verifying the goodness of the growth procedure and the 5 N optical purity of finished samples. The increase of background absorption visible in the spectra in Fig. 1 between 300 and 180 nm is not due to the host absorption, which is transparent in this region, but mainly to Rayleigh scattering from the surfaces. Even if the entrance and exit facets of the samples were polished before absorption measurements, surface roughness, and imperfections are still present and cause efficient scattering at short wavelength, increasing the background absorption in such region. The

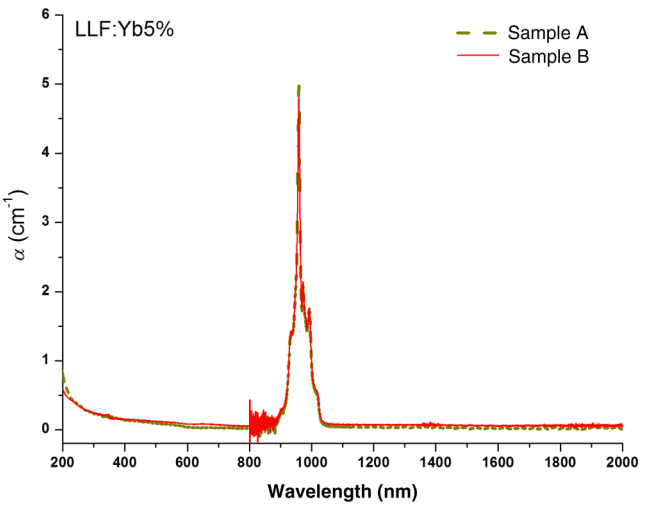

Fig. 1 Room-temperature unpolarized absorption spectra of samples A and B acquired between 200 nm and 2 μm to check for absence of major contaminants. The spectral resolution is 0.6 between 200 and 800 nm, and 0.8 nm between 800 nm and 2 μm.

automatic detector change of the spectrophotometer around 800 nm is the source of the noise in this region.

2.2 *Yb Spectroscopy*

Absorption and fluorescence spectra of the Yb transition were acquired in detail for both the LLF samples to verify the absence of appreciable differences in Yb optical properties between the two materials and, also, to measure the spectroscopic parameters which enter the model cooling efficiency curve, i.e., absorption coefficient and mean emission wavelength. The mean emission wavelength λ_f of the electronic transition, defined as

$$\lambda_f = \frac{\sum_i \int \lambda I_i(\lambda) \mathrm{d}\lambda}{\sum_i \int I_i(\lambda) \mathrm{d}\lambda},$$

where $I_i(\lambda)$ is the fluorescence spectrum relative to the i polarization, identifies the excitation region for the anti-Stokes process, i.e., $\lambda > \lambda_f$. The absorption coefficient, relatively low in this tail region $\lambda > \lambda_f$, is a parameter that needs to be maximized to minimize losses of pump power and rates of competing heat-generating impurities-mediated processes.

Absorption measurements were performed by means of a spectrophotometer Cary 5000 (Varian), operative between 180 and 3200 nm with 0.05 nm spectral resolution and 0.001 absorbance resolution. Room-temperature absorption spectra of both the LLF:5%Yb samples, for the two polarizations $E\|c$ and $E \perp c$, are shown in Fig. 2.

No appreciable differences in size and spectral distribution can be detected between the two LLF:Yb samples, within the experimental uncertainty. From the plot, it can be noticed that the $E\|c$ polarization allows the highest absorption coefficient, especially at long wavelengths, i.e., in the excitation region for the anti-Stokes process. Samples will be excited with E parallel to the c-axis in laser cooling experiments to maximize the absorption of pump power.

Fluorescence spectra were acquired by exciting the Yb transition at 940 nm with laser diode, and sampling the emission perpendicularly to the pump beam to reduce spurious scattering. The fluorescence was mechanically chopped

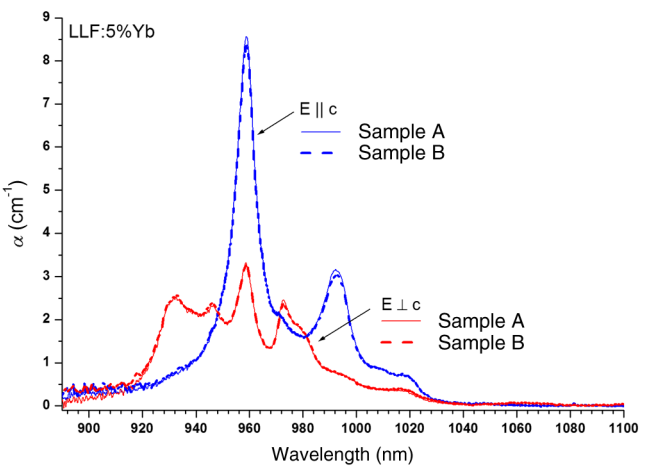

Fig. 2 Polarized absorption spectra of the two LLF:5%Yb samples investigated. Spectra were acquired with 0.3-nm spectral resolution.

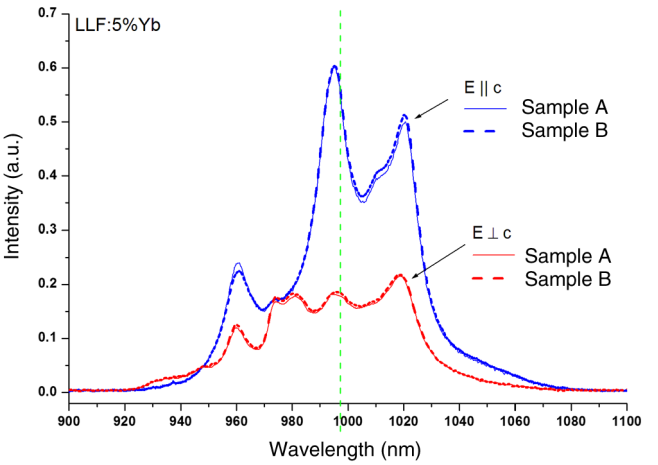

Fig. 3 Polarized fluorescence spectra of the two LLF:5%Yb samples. The green-dashed line indicates the mean emission wavelength. Spectra were acquired with 0.5-nm spectral resolution.

and collected by means of a monochromator, equipped with a 600-nm/mm diffraction grating (5.4-nm/mm dispersion), coupled to a photodiode InSb detector, placed at the output port. The detector output signal was processed by means of a lock-in amplifier, synchronized to the chopper frequency. A custom made holder, designed to place samples exactly at the same position, was used to obtain comparable intensity data of different samples. Raw fluorescence data were corrected for the spectral response of the experimental set-up measuring the emission spectra of a black-body source at 3000 K. Figure 3 shows fluorescence spectra of both the LLF:5%Yb samples, acquired in the same experimental conditions just replacing the sample on the holder. Even for emission, spectra of the two LLF:5%Yb overlap perfectly within the experimental uncertainty, and no appreciable differences can be detected between the two samples. Fluorescence spectra were used to evaluate the mean emission wavelength of the Yb transition, which resulted for both LLF samples around 997 nm.

3 Laser Cooling Measurements

Laser cooling performances of active media are normally evaluated by measuring the cooling efficiency spectrum at room temperature, defined as[14,15]

$$\eta_c(\lambda, T) = 1 - \eta_{\mathrm{ext}} \left[\frac{\alpha_r(\lambda, T)}{\alpha_r(\lambda, T) + \alpha_b} \right] \frac{\lambda}{\lambda_f(T)}, \quad (1)$$

where η_{ext} is the EQE of the electronic transition,[14] α_b is the background absorption coefficient of the material; and $\alpha_r(\lambda, T)$ and $\lambda_f(T)$ are the resonant absorption coefficient spectrum and the mean emission wavelength of the electronic transition, respectively. Net cooling occurs only if $\eta_c > 0$.

EQE and background absorption coefficient are the two parameters which quantify the cooling performances of the material under investigation. These parameters can be experimentally measured from fit of cooling efficiency data with the model curve in Eq. (1). Maximizing the cooling efficiency requires minimizing α_b and maximizing EQE. Background absorption is mainly related to unwanted impurities incorporated in active media from starting materials

and is currently the main parameter which limits the cooling performances of fluorides.[6] The EQE parameter, instead, is essentially related to the rate of nonradiative loss processes (phonon quenching, phonon-assisted impurities-mediated energy-transfer) and to the escape efficiency of fluorescence, limited by reabsorption and internal reflections.

For the laser cooling test, a standard single-pass set-up was used. The sample was mounted inside a vacuum chamber (evacuated down to 10^{-5} Pa), on a stainless steel holder, suspended on two optical fibers; in order to minimize convective and conductive heat loads. Four windows on the chamber walls enabled excitation and acquisition of the sample temperature simultaneously.

Contactless techniques are required to measure the sample temperature without altering its thermal capacity. A long-wavelength infrared thermal camera (Raytheon 2500AS) with microbolometer sensor was employed to acquire the IR fluorescence from the sample, through a BaF_2 window of the chamber, for temperature measurements. The thermal camera was previously calibrated to determine the relationship between pixel intensity and temperature variations and a linear response range of ±5°C was measured. For measuring the temperature change of the sample, a thermal video was acquired while the sample was under laser excitation. The video started with the absence of laser excitation and was extended until thermal equilibrium was reached. The stability of the chamber temperature was monitored by means of a thermocouple. Assuming that the main heat load on the sample is due to blackbody radiation, for relatively low temperature changes, the cooling power is proportional to the temperature difference between the sample and the environment.[6]

Optical cooling was observed for both samples under laser excitation at 1025 nm. A temperature drop of about 2°C was detected for both samples by exciting the Yb transition in single-pass at 1025 nm, with 220 mW of incident power and estimated absorbed power about 65 mW. Experimental data acquired for sample A are shown in Fig. 4. A similar behavior was detected for sample B.

For cooling efficiency measurements, the heating/cooling temperature change of the sample as a function of pumping wavelength was acquired. Four diode laser sources, with central wavelengths between 940 and 1060 nm, were used to excite the sample. All the junctions were mounted to excite the sample along the c-axis. Antireflection-coated BK7 windows were used to pass the laser beams trough the vacuum chamber. For each pumping wavelength, the temperature change was repeatedly measured several times with acquisition of thermal videos.

By measuring the heating/cooling temperature change as a function of pumping wavelength, similar cooling performances were detected for the two samples A and B. Experimental data points and fit model curves are shown in Fig. 5. EQE and background absorption coefficient have been estimated from fit of experimental data with the model curve in Eq. (1), obtaining the following values: $\mathrm{EQE} = 0.991 \pm 0.001$ and $\alpha_b = (1.5 \pm 0.2) \times 10^{-3}$ cm^{-1} for sample A, $\mathrm{EQE} = 0.990 \pm 0.001$ and $\alpha_b = (1.3 \pm 0.2) \times 10^{-3}$ cm^{-1} for sample B.

A maximum efficiency around 1.4% at 1025 nm was measured for both the LLF:5%Yb samples. Previous (and unique) literature data for laser cooling of LLF:Yb[12] only report a local estimation of cooling efficiency at 1015 nm, returning a value ~1.27%. However, these measurements were performed for an LLF:2%Yb in air for multipass laser excitation at single pumping wavelength; and the comparison is quite difficult as EQE and background absorption were not measured.

The fitted values of EQE and background absorption allow a comparison with the cooling performances of YLF[4,16]. Comparing these data, it can be noticed that LLF shows depressed cooling performances if compared to YLF doped at the same doping level. Such lower performances, however, can be basically related to the strong background absorption measured for LLF:5%Yb samples.

As the main source of parasitic absorption is impurities-mediated processes, we expect the lower cooling performances observed for the LLF samples to be essentially related to detrimental contaminants incorporated in the LLF samples, and not to intrinsic unfavorable properties of the LLF host. No appreciable difference, indeed, can be observed in Yb optical properties between YLF and LLF hosts. Simulations of cooling efficiency curve for LLF:5% Yb single crystals with background absorption coefficient of the same size of that measured for YLF:5%Yb samples[4,16],

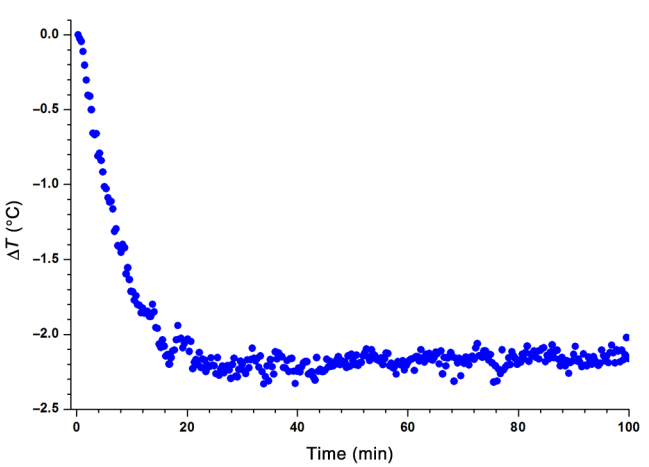

Fig. 4 Temporal evolution of temperature of LLF:5%Yb (sample A) under laser excitation in single-pass at 1025 nm, with 220 mW of incident power.

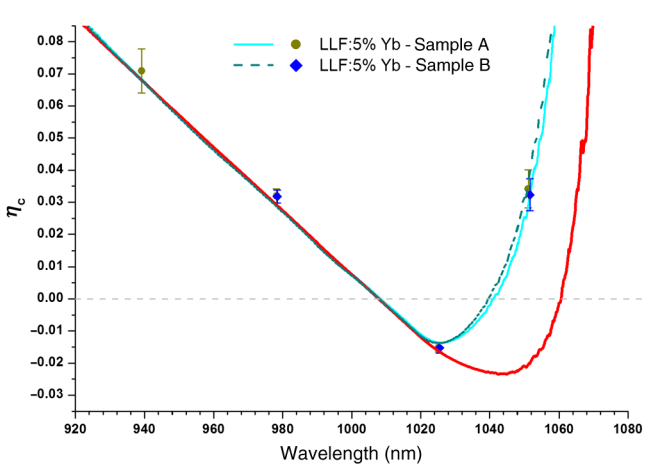

Fig. 5 Experimental data points measured for samples A and B, along with fit model curve. The red curve depicts the simulated cooling efficiency for LLF:5%Yb with EQE = 0.99 and $\alpha_b = 4.0 \times 10^{-4}$ cm^{-1}.

i.e., $\alpha_b \sim 4 \times 10^{-4}$ cm^{-1}, and EQE $= 0.990 \pm 0.001$ show comparable values of cooling efficiency for YLF and LLF samples, indication that the lower cooling performances measured for the LLF host are uncorrelated to the Yb spectroscopic properties but instead can be essentially related to impurities-mediated loss processes. The simulated cooling efficiency curve for LLF:5%Yb with EQE $= 0.99$ and $\alpha_b = 4 \times 10^{-4}$ cm^{-1} is reported in Fig. 5 for comparison with Ref. 4, and 16.

In addition to that, with the two samples grown in different laboratories, the similar values of background absorption measured for both samples provide evidence that the most detrimental impurities are introduced from starting materials and not by the handling of the growth process. For example, the same experimental set-up and procedures were used for the YLF:Yb sample set. However, much lower background absorption was measured for those samples, even if always starting from 5 N purity raw materials. Further investigations also showed samples of the same nominal composition (YLF:5%Yb, LLF:5%Yb) with equivalent Yb absorption and emission cross section just grown starting from different batches of starting materials, to show completely differences in cooling test, supporting the hypothesis that the main contaminations which affect the efficiency of the anti-Stokes process are those introduced from raw materials. Even though the optical purity of active materials is verified at the 10-ppm level, different relative concentrations of rare-earths and transition metals impurities are expected to be contained in different batches of raw materials and higher concentrations of some detrimental impurities can significantly reduce, or even compromise, the anti-Stokes cooling process. Results presented in this work, however, need further investigation to compare the efficiency of YLF and LLF hosts. Kinds and concentrations of impurities incorporated inside investigated samples need to be identified to quantify the effect of impurities-mediated process on the anti-Stokes efficiency and distinguish between host related effects and efficiency decreases related to due to impurities-mediated processes. Toward this end, a detailed impurities investigation via an elemental analysis of samples is underway.

4 Conclusions

In this work, we investigated the cooling performances of two different LLF:5%Yb samples measuring the room-temperature cooling efficiency curve from the heating/cooling temperature change as a function of pumping wavelength. High-quality LLF:5%Yb single crystals have been grown and optically characterized for the anti-Stokes process. Optical cooling has been observed for both samples exciting the Yb transition at 1025 nm. A temperature drop of 2.2°C with 220 mW of incident power in single-pass was detected and a peak cooling efficiency of about 0.015 at 1025 nm was measured. EQE and background absorption parameters have been estimated for both samples from fit of experimental data with the model curve.

Acknowledgments

The authors would like to acknowledge I. Grassini for her competence and care in preparing the samples. A. Volpi acknowledges support by the European Space Agency under Grant No. 4000108074/13/NL/PA—"Cooling effect on fluoride crystals." G. Cittadino acknowledges support by the European Space Agency under Grant No. 4000113313/15/NL/PA—"An increasing cooling efficiency in fluoride crystals codoped Yb-Tm."

References

1. R. I. Epstein et al., "Observation of laser-induced fluorescent cooling of a solid," *Nature* **377**, 500–503 (1995).
2. D. V. Seletskiy et al., "Laser cooling of solids to cryogenic temperatures," *Nat. Photonics* **4**, 161–164 (2010).
3. S. D. Melgaard et al., "Optical refrigeration to 119 K, below National Institute of Standards and Technology cryogenic temperature," *Opt. Lett.* **38**, 1588–1590 (2013).
4. S. D. Melgaard et al., "Identification of parasitic losses in Yb:YLF and prospects for optical refrigeration down to 80 K," *Opt. Exp.* **22**, 7756–7764 (2014).
5. S. D. Melgaard et al., "Solid-state optical refrigeration to sub-100 Kelvin regime," *Sci. Rep.* **6**, 20380 (2016).
6. S. D. Melgaard, "Cryogenic optical refrigeration: laser cooling of solids below 123 K," PhD Dissertation, University of New Mexico, Albuquerque, NM (2013).
7. S. Bigotta et al., "Single fluoride crystals as materials for laser cooling applications," *Proc. SPIE* **6461**, 64610E (2007).
8. I. M. Ranieri et al., "Growth of $LiY_{(1-x-y)}Lu_xNd_yF4$ crystals for optical applications," *J. Cryst. Growth* **209**, 906–910 (2000).
9. H. Yu et al., "Compact passively Q-switched diode-pumped Tm:$LiLuF_4$ laser with 1.26 mJ output energy," *Opt. Lett.* **37**, 2544–2546 (2012).
10. J. G. Yin et al., "Direct comparison of Yb^{3+}-doped $LiYF_4$ and $LiLuF_4$ as laser media at room-temperature," *Laser Phys. Lett.* **9**, 126–130 (2012).
11. B. M. Walsh et al., "Spectroscopy and modeling of solid state lanthanide lasers: application to trivalent Tm^{3+} and Ho^{3+} in $YLiF_4$ and $LiLuF_4$," *J. Appl. Phys.* **95**, 3255–3271 (2004).
12. B. Zhong et al., "Laser cooling of Yb^{3+}-doped $LuLiF_4$ crystal," *Opt. Lett.* **39**, 2747–2750 (2014).
13. B. Pamplin, *Crystal Growth*, Pergamon Press, Oxford (1975).
14. M. Sheik-Bahae and R. I. Epstein, "Optical refrigeration," *Nat. Photonics* **1**, 693–699 (2007).
15. D. V. Seletskiy et al., "Cryogenic optical refrigeration," *Adv. Opt. Photonics* **4**, 78–107 (2012).
16. A. Volpi, A. Di Lieto, and M. Tonelli, "A novel approach for solid-state cryoccolers," *Opt. Exp.* **23**, 8216–8226 (2015).

Biographies for the authors are not available.